HHS Public Access

Author manuscript

Biotechnol J. Author manuscript; available in PMC 2018 November 01.

Published in final edited form as:

Biotechnol J. 2017 November ; 12(11): . doi:10.1002/biot.201600751.

Exploring bacterial carboxylate reductases for the reduction of bifunctional carboxylic acids

Anna N. Khusnutdinova[1], **Robert Flick**[1], **Ana Popovic**[1], **Greg Brown**[1], **Anatoli Tchigvintsev**[1], **Boguslaw Nocek**[2], **Kevin Correia**[1], **Jeong Chan Joo**[3], **Radhakrishnan Mahadevan**[1], and **Alexander F. Yakunin**[1]

[1]Department of Chemical Engineering and Applied Chemistry, University of Toronto, 200 College Street, ON M5S 3E5, Canada

[2]Midwest Center for Structural Genomics and Structural Biology Center, Biosciences Division, Argonne National Laboratory, Argonne, Illinois 60439, USA

[3]Center for Bio-based Chemistry, Division of Convergence Chemistry, Korea Research Institute of Chemical Technology, 141 Gajeong-ro, Yuseong-gu, Daejeon 34114, Republic of Korea

Abstract

Carboxylic acid reductases (CARs) selectively reduce carboxylic acids to aldehydes using ATP and NADPH as cofactors under mild conditions. Although CARs have attracted significant interest, only a few enzymes have been characterized to date, whereas the vast majority of CARs have yet to be examined. Herein we report that 12 bacterial CARs reduced a broad range of bifunctional carboxylic acids containing oxo-, hydroxy-, amino-, or second carboxyl groups with several enzymes showing activity toward 4-hydroxybutanoic (4-HB) and adipic acids. These CARs exhibited significant reductase activity against substrates whose second functional group is separated from the carboxylate by at least three carbons with both carboxylate groups being reduced in dicarboxylic acids. Purified CARs supplemented with cofactor regenerating systems (for ATP and NADPH), an inorganic pyrophosphatase, and an aldo-keto reductase catalyzed a high conversion (50–76%) of 4-HB to 1,4-butanediol (1,4-BDO) and adipic acid to 1,6-hexanediol (1,6-HDO). Likewise, *Escherichia coli* strains expressing eight different CARs efficiently reduced 4-HB to 1,4-BDO with 50–95% conversion, whereas adipic acid was reduced to a mixture of 6-hydroxyhexanoic acid (6-HHA) and 1,6-HDO. Thus, our results illustrate the broad biochemical diversity of bacterial CARs and their compatibility with other enzymes for applications in biocatalysis.

Graphical abstract

Carboxylic acid reductases (CAR) reduce carboxylic acids to aldehydes using ATP and NADPH as cofactors. In this work, the authors demonstrated that 12 bacterial CARs can reduce a broad range of bifunctional carboxylic acids. Several CARs catalyzed a high conversion of 4-hydroxybutanoic

Correspondence: Dr. Alexander Yakunin, Department of Chemical Engineering and Applied Chemistry, University of Toronto, 200 College Street, Toronto, Ontario, M5S 3E5, Canada. a.iakounine@utoronto.ca.

Conflict of interest

The authors declare no financial or commercial conflict of interest.

and adipic acids to 1,4-butanediol, 1,6-hexanediol, and 6-hydroxyhexanoic acid *in vitro* (in combination with cofactor regenerating systems and aldo-keto reductases) and *in vivo* (in *E. coli* cells).

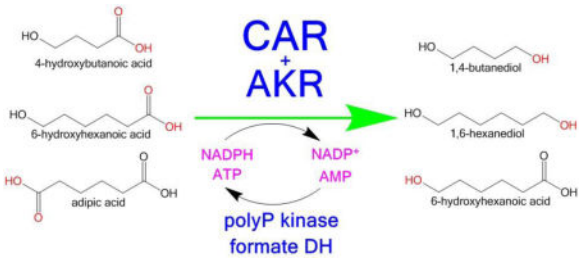

Keywords

adipic acid; 1,4-butanediol; carboxylic acid reductase; 1,6-hexanediol; 4-hydroxybutyrate

1 Introduction

The depletion of global fossil fuel resources and the high CO_2 emissions from their use creates the demand for efficient substitution of petroleum by renewable feedstocks. Biotechnological production of valuable chemicals and biofuels from renewable sources has been receiving increased attention as an alternative to petroleum-based refinery processes [1–3]. Organic acids serve as precursors for a variety of bulk chemicals and important polymers whose significance for the chemical industry has been underlined by the US Department of Energy, which has included nine organic acids into the list of the top 12 value-added platform chemicals [1, 4]. In addition, many chemical transformations involve substrates or intermediates containing carboxylic groups, which are reduced to aldehydes with the aid of expensive and environmentally harmful chemical processes [5]. Enzyme-catalyzed reduction of carboxylic groups offers the typical advantages of biocatalytic processes including mild reaction conditions, chemoselectivity, and enantioselectivity. Bio-based production of organic acids has become a fast-moving field due to the recent advances in genome sequencing, metabolic engineering and synthetic biology [6, 7]. Bifunctional carboxylic acids (di-acids, hydroxy-acids, oxo-acids, and amino-acids) are of special interest in the polymer industry because they are components of different bio-based polymers (polyesters and polyamides) [2, 8]. In industrially important microorganisms, bifunctional carboxylic acids (succinate, malate, fumarate, 2-oxoglutarate, etc.) are intermediates of the central carbon metabolism representing potential starting points for the biosynthesis of various chemicals. The growing bio-based production of organic acids from renewable sources makes them attractive substrates for a range of alternative products [5, 8]. Therefore, biocatalytic reduction of carboxylic acids is gaining importance [9].

Thermodynamically, the reduction of carboxylic acids is very unfavorable and difficult to perform biocatalytically [9, 10]. Nevetheless, there are many reports on the aerobic and anaerobic biocatalytic reduction of various aromatic and aliphatic carboxylic acids by fungi, bacteria, and archaea [5]. Nearly all of these works were performed using resting or growing cells of native or recombinant organisms or their crude extracts. Thus, the majority of

enzymes responsible for these reactions remain to be identified and characterized in order to assess their potential as industrial biocatalysts [5]. Biochemical characterization of several purified enzymes has revealed the presence of at least two different enzyme families: aldehyde oxidoreductases (AORs; EC 1.2.99.6) from anaerobic bacteria and archaea and carboxylate reductases (CARs; EC 1.2.1.30) from aerobic organisms [5]. Mo- or W-containing AORs from clostridia or thermophilic archaea are very labile oxygen-sensitive iron-sulfur proteins, which use reduced ferredoxin or methyl viologen as electron donors [11, 12]. In contrast, the purified CARs from *Neurospora crassa* and two *Nocardia* strains were insensitive to oxygen and required NADPH and ATP for activity [13–15]. Further work showed that these enzymes catalyze the initial reaction between ATP and a substrate acid to form an acyl-AMP intermediate, which is then reduced by NADPH to form the aldehyde product [16, 17]. Heterologous expression of the *N. iowensis* CAR in *Escherichia coli* provided an opportunity to further explore its molecular properties and carboxylate reductase activity [18]. Biochemical studies with the purified *N. iowensis* CAR revealed a large monomeric protein (over 1,000 amino acids) containing an N-terminal AMP-binding (or adenylating) domain and a C-terminal NADPH-binding domain with a phosphopantetheine attachment site located between them [17–19]. For maximal enzyme activity, the recombinant *N. iowensis* CAR required post-translational activation via phosphopantetheinylation by a phosphopantetheinyl transferase (PPT, co-expressed in *E. coli* or added as a purified protein) [19]. The proposed catalytic model of CAR-catalyzed reduction of benzoic acid suggests that the deprotonated acid is first activated by ATP at the adenylating domain with the formation of adenosyl phosphate, which is then nucleophilically attacked by the phosphopantetheine thiol forming a covalently bound benzoyl thioester with the release of AMP [19]. The benzoyl thioester-phosphopantetheinyl arm then swings from the adenylating domain to the C-terminal reduction domain resulting in the reduction of the thioester by NADPH releasing benzaldehyde, $NADP^+$, and free enzyme.

Purified CARs from *Neurospora* and *Nocardia* have been shown to accept a wide variety of aryl carboxylic acids as substrates including benzoic acid and its derivatives, as well as several aliphatic carboxylic acids [13–16, 20, 21]. Recently, a similar substrate preference was also demonstrated for the purified CARs from *Mycobacterium marinum*, which exhibited high catalytic efficiency (k_{cat}/K_m) against benzoic acid and the C_8-C_{12} fatty acids [22]. Significant carboxylate reductase activity with aromatic substrates was also found in the purified recombinant CARs from *Segniliparus rotundus*, *N. brasiliensis*, *N. otitidiscaviarum*, *M. smegmatis*, *M. phlei*, and *N. crassa* [23–26]. Several successful applications of the *N. iowensis* and *M. marinum* CARs have already been demonstrated for the microbial production of alkanes, propane, and aromatic aldehydes [21, 22, 26–29]. The observed broad substrate scope and kinetic characteristics of these CARs suggest the potential for their future development as industrial biocatalysts [5, 22, 30].

Despite the high interest in biocatalytic applications of CARs, their biochemical properties and substrate scope have not been examined in depth. The vast majority of microbial CARs remain uncharacterized including their phylogeny, biochemical diversity, and kinetic properties, which limits the scope of their applications. In addition, the applicability of CARs for the reduction of bifunctional carboxylic acids (diacids, hydroxyacids, oxoacids,

amino acids), which are important intermediates in the polymer industry, remains to be explored. Here we present a detailed analysis of 15 bacterial CARs including their substrate profiles and activities toward bifunctional carboxylic acids. Using purified CARs in combination with aldo-keto reductases (AKRs) and cofactor regenerating systems, we have demonstrated the applicability of CARs for the *in vitro* reduction of 4-hydroxybutanoic acid (4-HB) to 1,4-butanediol (1,4-BDO) and adipic acid to 1,6-hexanediol (1,6-HDO) with up to 90% substrate conversion. Similar substrate conversion efficiencies were also observed for the *in vivo* reactions using *Escherichia coli* cells expressing different recombinant CARs. This work provides further insights into the biochemical diversity and biocatalytic potential of bacterial CARs.

2 Materials and methods

2.1 Phylogenetic analysis

The phylogenetic tree was generated using the MAB4714 CAR sequence, which retrieved 772 sequences with the same domain organization from the Conserved Domain Architecture Retrieval Tool (CDART; https://www.ncbi.nlm.nih.gov/Structure/lexington/lexington.cgi?cmd=rps/) [31]. The original dataset was reduced to 598 sequences by removing redundant sequences and increasing gap-free sites using CD-HIT [32] and MaxAlign [33] within the MAFFT online alignment tool [34] (http://mafft.cbrc.jp/alignment/server/). The tree was built using 100 iterations and a 60% threshold value for bootstraps. The neighbor-joining tree of 20 bacterial CARs cloned in this work was generated using Geneious 6.0.6 with 100 iterations and bootstrap values > 60%.

2.2 Gene cloning and protein purification

The genes encoding 20 selected CARs and other proteins (aldo-keto reductases, polyphosphate kinases PA3455 from *Pseudomonas aeruginosa* and Smc02148 from *Sinorhizobium meliloti*) (Table S1) were amplified by PCR from corresponding genomic DNA and cloned into a modified pET15b vector (Novagen) containing an N-terminal 6His-tag as described previously [35]. The phosphopantetheinyl transferases (PPTs) BSU03579 (Sfp) from *Bacillus subtilis* and EntD from *E. coli* were cloned into a pCDFDuet plasmid for co-expression with CARs. The plasmids were transformed into the expression host *E. coli* BL21(DE3) Gold strain (Agilent). Recombinant proteins were over-expressed and purified to homogeneity (>95%) using metal-chelate affinity chromatography on Ni-NTA Superflow resin (Qiagen) (Figure S1) [35]. Site-directed mutagenesis of the *Pseudomonas* sp. strain 101 formate dehydrogenase (FDH, P33160) was performed using the QuikChange™ site-directed mutagenesis kit (Stratagene) according to the manufacturer's protocol, and the mutations (D222Q/H224N) were verified by DNA sequencing.

2.3 Enzymatic assays and reaction product analysis

Carboxylate reductase activity of purified CARs against different carboxylic acids and aldehyde reductase activity of purified AKRs were determined spectrophotometrically using an NADPH oxidation-based assay by following the decrease in absorbance at 340 nm. CAR screening was performed in a reaction mixture (0.2 ml) containing HEPES-K (100 mM, pH 7.5), 1 mM NADPH, 2.5 mM ATP, 10 mM $MgCl_2$, 10 mM substrate (5 mM for decanoic

acid), and 2.5 – 5.0 μg of purified CAR (10 min incubation at 30°C). AKR screening was carried out in a reaction mixture containing 50 mM HEPES-K (pH 7.5), 0.5 mM NADPH or NADH, 10 mM butyraldehyde or adipaldehyde, and 2 μg of purified AKR (10 min incubation at 30°C). The pH dependence of reductase activity of purified CARs and AKRs was determined using a mixed buffer system (MEGA buffer) [36]. The kinetic experiments for the determination of K_m and k_{cat} were performed using a microplate-based assay (0.2 ml) in triplicate in a reaction mixture containing a range of variable substrates (0.025 – 50 mM). Kinetic parameters were determined by non-linear curve fitting from the Lineweaver-Burk plot using GraphPad Prism (version 5.00 for Windows, GraphPad Software, San Diego, CA).

The reaction products of the CAR and AKR catalyzed bioconversions were quantified using a Varian ProStar HPLC system equipped with an Aminex HPX-87H column (300 × 7.8 mm; Bio-Rad) and Varian PDA (model 330) and RI (model 350) detectors. Reaction mixtures and culture supernatants were filtered through 10 kDa spin filters (PES membrane, VWR) and eluted using 5 mM H_2SO_4 as the running buffer (0.5 ml/min, 50°C). Concentrations of substrates and products for *in vivo* and *in vitro* biotransformations were determined using linear regression analysis of the refractive index peak areas (with subtracted control sample areas). Results are means ± SEM (standard error of mean) from at least three independent determinations.

PolyP kinase reactions with the indicated PPK2 proteins were performed using 5 mM polyP (sodium polyphosphate crystals, +80 mesh, FW ~1286, Aldrich cat # 305553) and 5 mM AMP or 5 mM ADP as substrates. The reaction products (ADP and ATP) were analyzed using reversed phase chromatography on a Varian ProStar HPLC system equipped with a Varian Pursuit C18 column as previously described [37, 38]. Standard solutions of AMP, ADP, and ATP were used to confirm the identity of the observed peaks and products. Formate-dependent reduction of NAD^+ and $NADP^+$ by the D222Q/H224N double mutant FDH from *Pseudomonas* sp. strain 101 (Uniprot ID P33160) was followed at 340 nm [39]. Reaction mixtures contained 100 mM Tris-HCl (pH 8.0), 50 mM formate, and 1 μg of purified mutant FDH.

Liquid chromatography-mass spectrometry (LC-MS) analysis of CAR reaction products (1,4-BDO, 1,6-HDO, and 6-HHA) was performed using a Dionex Ultimate 3000 UHPLC system and a Q-Exactive mass spectrometer equipped with a HESI source (all from Thermo Scientific) and controlled by Thermo XCalibur 2.2 software. LC separation was conducted on a Hypersil Gold C18 column (50 mm × 2.1 mm, 1.9 μ particle size, Thermo Scientific) equipped with a guard column. Solvent A was 0.1% formic acid (in water), solvent B was 0.1% formic acid in methanol (flow rate 0.2 ml/min). Autosampler temperature was maintained at 8°C, and injection volume was 10 μl. The gradient was 0 – 2.5 min: 100% A; 2.5 – 4.5 min: 15% A, 85% B; 4.5 – 8.0 min: 15% A, 85% B; 8.0 – 8.5 min: 100% A; 8.5 – 12 min: 100% A. Data collection was done in positive ionization mode with a scan range m/z 100–300, resolution 70000 at 1 Hz, AGC target of 3e6 and a maximum injection time of 200 ms. Standard solutions of 1,4-BDO (m/z 91.0769), 1,6-HDO (m/z 119.1062), and 6-HHA (m/z 133.0864) were used for validation of retention time and m/z.

2.4 *In vitro* and *in vivo* biotransformations of 4-HB and adipic acid

In vitro biotransformations without cofactor regeneration were carried out in reaction mixtures (0.2 ml) containing 100 mM HEPES-K buffer (pH 7.5), 10 mM substrate (4-HB or adipic acid), 3 mM NADPH, 5 mM ATP, 10 mM $MgCl_2$, 80 μg of purified CAR (or Ni column elution buffer in control reactions) and 20 μg of purified AKR (PP3340) (overnight at 30°C, 800 rpm). Biotransformations with the addition of cofactor regenerating systems and inorganic pyrophosphatase were performed in the presence of 100 mM HEPES-K buffer (pH 7.5), 10 mM substrate (4-HB or adipic acid), 2 mM NADPH, 2 mM ATP, 2 mM polyP, 20 mM $MgCl_2$, 60 mM Na-formate, 10 μg PA3455, 10 μg SMc02148, 20 μg of the D222Q/H224N formate dehydrogenase (P33160), 10 μg of the *E. coli* inorganic pyrophosphatase (PPase). After a 12 h incubation, the reaction mixtures were filtered through 10 kDa spin filters (PES membrane, VWR) and the reaction products were analyzed using HPLC or LC-MS.

In vivo biotransformations were carried out using *E. coli* BL21(DE3) cells expressing the indicated CAR proteins and BSU03570 (the phosphopantetheinyl transferase Sfp) on separate plasmids. The overnight starter cultures were diluted with fresh LB medium containing 2% glucose (to $A_{600} < 0.1$) and grown aerobically at 37°C up to a cell density of $A_{600} = 0.6$ followed by the addition of 10 mM substrate (4-HB or adipic acid) and 0.2 mM IPTG. Culture aliquots (0.3 ml) were collected at the indicated times and the reaction products (in culture supernatants) were analyzed using HPLC as described above. *E. coli* BL21(DE3) Gold cells transformed with an empty modified pET15b vector were used as controls.

3 Results and Discussion

3.1 Phylogenetic analysis of CARs

Sequence analysis of the biochemically characterized CARs from *N. iowensis* and *M. marinum* revealed the presence of three protein domains: the N-terminal adenylation domain (PF00501), the phosphopantetheine attachment site (PF00550), and the C-terminal $NADP^+$ reductase domain (PF07793) (Figure 1A) [19, 22]. To obtain insight into the phylogenetic diversity of CARs, we extracted over 3,700 homologous sequences from GenBank. By excluding redundant and degenerate/incomplete sequences, this pool of potential CARs was reduced to 1,755 proteins including many sequences in Fungi (Ascomycota and Basidiomycota), as well as in Actinobacteria, Firmicutes, and Proteobacteria. Similar to the recently published phylogenetic analysis [40], we found that bacterial and fungal CARs fall into different groups. Phylogenetic analysis of the prokaryotic CAR sequences revealed that they are present both in Gram-positive and Gram-negative bacteria and form at least five monophyletic groups (CAR1 to CAR5) (Figure 1B). The unrooted tree of prokaryotic CARs shows the presence of the four major clades including CAR1 (Corynebacteriales, Streptomycetales, Terrabacteria), CAR2 (Bacillales, Terrabacteria), CAR3 (Pseudomonadales, γ-Proteobacteria), and CAR4 (a mixed group, mainly Enterobacteriales), whereas the minor group CAR5 includes Burkholderiales (β-Proteobacteria) (Figure 1B). The biochemically characterized CARs from *N. iowensis* (CAR_NOCIO) [19] and *M. marinum* (MMA2117) [22] belong to the CAR1 group, which

is the main focus of this study. The CAR1 group also includes the recently analyzed 48 CAR sequences from the families Streptomycetales and Corynebacteriales [25]. Phylogenetic analysis of the 20 cloned CARs (Table 1) from the CAR1 group indicates that they form four separate clades (sub-groups) with CAR_NOCIO and MMA2117 located in the sub-groups I and IV, respectively (Figure 1C). In addition, many genomes from this group encode two to four CAR proteins (paralogues) with varying sequence similarity (50 – 90 % sequence identity) suggesting that they might have different substrate preferences.

3.2 CAR expression and screening

To explore the biochemical diversity of bacterial CARs from the major phylogenetic group CAR1 (Figure 1), 20 CAR genes from different Gram-positive bacteria (*Mycobacteria*, *Nocardia*, and *Segniliparus*, 48.4–94.4 % of sequence identity, Table S2) were cloned for recombinant expression in *E. coli* (without codon optimization). For maximal activity [19], the cloned CARs were co-expressed with a phosphopantetheinyl transferase (PPT) from *Bacillus subtilis* (BSU03570 or Sfp) or *E. coli* (EntD) (expressed from a pCDFduet plasmid). Recombinant expression and affinity purification yielded 15 soluble CAR proteins (4–40 mg/L *E. coli* culture) suggesting that codon optimization is not necessary for the preparative expression and purification of these large proteins (over 1,000 amino acids) (Table S1, Figure S1). Using benzoic acid as a common CAR substrate [14, 22], the 15 purified proteins were screened for the presence of reductase activity using an NADPH-oxidation assay. As shown in Figure 2A, 13 purified CARs showed detectable or significant reductase activities toward benzoic acid (0.25–1.7 U/mg). MSM2108 was found to be inactive, most likely due to the presence of a degenerate adenylation domain (Figure S2). Co-expression of CARs with PPTs had no considerable effect on the yield of purified protein, but increased their benzoic acid reductase activity 2–5 times (Figure S3). Like the previously characterized *N. iowensis* CAR_NOCIO [14], the novel CARs preferred NADPH over NADH as reductant, pH 7.0–7.5, and required the addition of ATP and Mg^{2+} (saturating at 0.5 mM and 10 mM, respectively) (data not shown). The apparent K_m and k_{cat} values of purified CARs for ATP, NADPH, and benzoic acid were found to be close to the previously characterized *N. iowensis* and *M. marinum* CARs (Table 2) [14, 22]. Thus, screening of 15 purified CARs revealed high and significant reductase activity against benzoic acid in 12 proteins.

3.3 Substrate scope of purified CARs

To provide insight into the substrate scope of bacterial CARs and their activity toward bifunctional carboxylic acids, the 15 purified proteins were screened for reductase activity against 87 substrates with different chain lengths including mono-, di-, hydroxy-, oxo-, and aminated carboxylic acids using a NADPH oxidation-based assay (Table S3). These screens revealed remarkably broad and overlapping substrate spectra in 12 CARs (except for MAB3367) with the highest catalytic activity (for the best substrate) observed in MAB4714, which was almost five times more active than the previously characterized MMA2117 from *M. marinum* [22] (Figure 3). In addition, MAB2962, MCH22995, MIM0040, and NBR0960 were 2–3 times more active than MMA2117 and displayed a broader substrate range (Figure 3). Pentanoic (valeric) acid (C5) was found to be the best substrate for MIM3725, whereas all other CARs showed a preference for cinnamic acid followed by benzoic acid. These

results suggest that purified CARs prefer substrates with a C2 linker between the carboxyl group and aromatic ring. While MAB4714, MMA2117, MAP1040, and SRO1679 showed a clear preference for cinnamic acid, other CARs (e.g. MIM0040, MIM3725, MSM2956, and MSM5739) exhibited prominent substrate promiscuity with similar levels of activity toward 5–15 substrates (Figure 3). Additionally, purified paralogous CARs (e.g. MAB2962 and MAB4714 or MSM2956, MSM5586, and MSM5739) revealed minor differences in substrate preference against the substrates used in this work (Figure 3). Thus, the identified bacterial CARs utilize a broad range of substrates including aliphatic and aromatic mono- and dicarboxylic acids, as well as hydroxy-, oxo-, and amino acids.

With mono-carboxylic acids as substrates, the purified CARs demonstrated significant reductase activity against C3-C10 substrates with the maximal activity toward C5-C7 acids (Figure 4). For a sub-set of 15 C4-carboxylic acids with various modifications, most of the purified CARs showed substantial reductase activity against substrates with the polar surface area 37 $Å^2$ (butanoic and 2-butenoic acids) (Figure S4). However, their activity was greatly diminished when the substrate polar surface area was increased to 54–89 $Å^2$ by the addition of hydroxy-, oxo-, or amino groups (Figure S4). Interestingly, the sub-group II CARs MAB4714 and SRO1679 exhibited significant reductase activity against 4-hydroxybutanoic acid (4-HB), which is a valuable commodity chemical.

The addition of a second carboxylic group to monocarboxylic acids with different chain lengths (C3-C10) had no effect on CAR activity with the long chain substrates (C8-C10), but reduced their activity against C6-C7 substrates (Figure 4). Nevertheless, the sub-group II CARs (MAB4714, MCH22995, and MIM0040) showed detectable reductase activity against adipic and *trans, trans*-muconic acids (both are C6 dicarboxylic acids). However, these enzymes were much less active toward the *cis,cis* isomeric form of muconic acid suggesting structural constraints with this unsaturated substrate geometry (Figure 4). Further truncation of the dicarboxylic acid chain length to C3-C5 resulted in a complete loss of CAR activity (Figure 4). Similarly, the addition of an amino group to carboxylic acids reduced or eliminated the reductase activity of all purified CARs against the C5-C7 substrates, but the subgroup II CARs (MAB4714, MCH22995, and MIM0040) retained significant catalytic activity against 9-aminononanoic and 10-aminodecanoic acids (Figure 4). These results indicate that the presence of the second charged (positive or negative) or polar group close to the substrate carboxylic group has a negative effect on CAR activity. Nevertheless, CARs can accept bifunctional carboxylic acids as substrates if the second charged group is located 5–7 carbon atoms away from the substrate carboxylic acid. Overall, the substrate range of bacterial CARs is not limited to mono-carboxylic acids, and they tolerate the presence of a second charged or polar group in their substrates making them useful for the biocatalytic transformation of bifunctional carboxylic acids.

3.4 *In vitro* biotransformation of 4-HB and adipic acid by purified CARs

Screening of the purified CARs revealed that several enzymes exhibit detectable reductase activity against 4-HB and adipic acid (Figures 2B, 4, and S4). Although CARs showed lower affinity (higher K_m) to these substrates compared to benzoic acid, their apparent catalytic rates (k_{cat}) were in the same range (0.4 – 4.5 s^{-1}) (Table 2). Therefore, we explored the

possibility of using these enzymes in combination with aldo-keto reductases (AKR) as biocatalysts for the production of corresponding diols, 1,4-butanediol (1,4-BDO) and 1,6-hexanediol (1,6-HDO) (Figure 5). Both 1,4-BDO and 1,6-HDO are important commodity chemicals, with high annual demand, that are produced on a large scale of several million tons per year and are widely used for the production of plastics, polyurethanes and pharmaceuticals [2, 4]. In addition, 1,6-HDO can be converted by amination to 1,6-hexamethylenediamine, another important chemical in the polymer industry [8]. The recently demonstrated biosynthetic pathway from glucose through succinate to 1,4-BDO proceeds via 4-HB, which is then converted to 1,4-BDO using three different enzymes [41]. In contrast, no biosynthetic pathway has been proposed for 1,6-HDO, which is currently produced industrially by the chemical hydrogenation of adipic acid. We propose that, using CARs and AKRs, the biosynthesis of 1,4-BDO from 4-HB can be shortened to two reactions, whereas adipic acid can be converted to 1,6-HDO (Figure 5). In combination with the recently demonstrated biosynthetic pathway for the conversion of glucose to adipic acid using an engineered *E. coli* strain [42], these CAR+AKR reactions can establish the first biosynthetic pathway for 1,6-HDO.

To identify novel NADPH-dependent AKRs suitable for the proposed CAR-catalyzed biotransformations (the reduction of 4-hydroxybutanal, 6-oxohexanoic acid, and 6-hydroxyhexanal), we screened our collection of 28 uncharacterized AKRs for reductase activity against butanal (as a substitute for 4-hydroxybutanal [41], which is not available commercially) and adipaldehyde using a mixture of NADPH and NADH as cofactors. These assays revealed detectable reductase activity against both substrates in six AKR proteins with the highest activity shown by the *Pseudomonas putida* PP3340 (Figure S5). Based on the analysis of kinetic parameters of identified AKRs against butanal and adipaldehyde (Table S4), PP3340 exhibited the highest catalytic efficiency (k_{cat}/K_m) in the NADPH-dependent reduction of both substrates, which was also higher than that of the most active CAR, MAB4714. Therefore, PP3340 was selected for applications in CAR-catalyzed biotransformations.

Using a HPLC-based assay for the analysis of reaction products, we examined the transformation of 4-HB and adipic acid to their corresponding diols by the eight purified CARs from the sub-groups II, III, and IV in the presence of PP3340, as well as ATP and NADPH as cofactors. After overnight incubation with 10 mM 4-HB, all CARs produced similar concentrations of 1,4-BDO (~1 mM) resulting in 10 % conversion (Figure 6A). With 10 mM adipic acid as substrate, MCH22995 and MIM0040 produced small amounts (0.2 – 0.3 mM) of 6-hydroxyhexanoic acid (6-HHA), whereas SRO1679 generated up to 0.5 mM 1,6-HDO as the final product (Figure 6B). The other five CARs synthesized approximately equimolar mixtures of both products with the highest total product level demonstrated by MAB4714 (~ 1.2 mM) (Figure 6B). The formation of these reaction products was confirmed using LC-MS (Figure S6). Thus, our results indicate that bacterial CARs can reduce both carboxylic groups in dicarboxylic acids. Relatively low *in vitro* conversion efficiency of 4-HB and adipic acid by purified CARs might be due to a limitation caused by cofactor exhaustion (3 mM NADPH and 5 mM ATP) and pyrophosphate inhibition [43] that can be resolved using cofactor regenerating systems and inorganic pyrophosphatase.

3.5 Complementation of CAR-catalyzed *in vitro* biotransformations with cofactor regenerating systems and inorganic pyrophosphatase

Biocatalytic reactions depending on ATP and nicotinamide cofactors require regenerating systems to restore the consumed cofactors. Currently, several enzyme-coupled systems have been proposed for the regeneration of NADPH and ATP [44–47]. To increase the substrate conversion efficiency of the *in vitro* CAR biotransformations, we established two cofactor regenerating systems for the regeneration of ATP from AMP (for CARs) and NADPH from $NADP^+$ (for both CARs and AKRs) (Figure 5). For the regeneration of NADPH in CAR-catalyzed reactions, we used the NAD-dependent formate dehydrogenase (FDH) from *Pseudomonas* sp. strain 101 (Uniprot ID P33160), into which we introduced two mutations: D222Q and H224N. Previously, it had been shown that these mutations change the cofactor preference of FDH from NADH to NADPH [39]. As presented in Figure S7A, in the presence of $NADP^+$ the purified D222Q/H224N FDH showed almost 10 times higher rates of formate oxidation to CO_2 than with NAD^+ making it useful for CAR-catalyzed biotransformations.

For the regeneration of ATP from ADP and AMP, several enzymatic reactions have been proposed including systems comprised of acetyl phosphate/acetate kinase, phosphoenolpyruvate/pyruvate kinase, and adenylate kinase/polyphosphate/polyphosphate kinase (AdK/polyP/PPK) [46]. In our previous work, we demonstrated that the polyP kinase PA3455 from *P. aeruginosa* (PPK2 subfamily-2) catalyzes mainly polyphosphate-dependent phosphorylation of AMP to ADP, whereas the PPK2 subfamily-1 enzyme SMc02148 from *Sinorhizobium meliloti* uses polyP to generate ATP from ADP [37]. In this work, the combination of PA3455 and SMc02148 transformed.

5 mM AMP to ATP after 1-hour incubation in the presence of 2 mM polyP (Figure S7B). In addition, we demonstrated the complete polyP-driven conversion of 5 mM AMP to ATP by the purified subfamily-3 PPK2 enzyme AAur_2811 from *Arthrobacter aurescens* (Figure S7B). In the presence of saturating concentrations of polyP (2 mM; K_m 21 – 62 μM), the three PPK2 enzymes showed high catalytic rates with AMP and ADP (k_{cat} 7.6 – 44.6 s^{-1}) with K_m in the range 0.03 – 0.8 mM corroborating their application for the regeneration of ATP from AMP or ADP (Figure S7B).

The addition of both regenerating systems to the 4-HB (10 mM) biotransformation reactions catalyzed by eight purified CARs in the presence of PP3340 increased the yields of 1,4-BDO for MAB4714, MAP1040, and MSM5586 more than two times resulting in 33% substrate conversion (up to 0.3 g/L for MAB4714), whereas other CARs showed no increase (Figure 6C). Similarly, the addition of these regenerating systems significantly increased the conversion of adipic acid (10 mM) to 1,6-HDO by MAB4714, MAP1040, and MSM5586 resulting in 25 – 40% substrate conversion (up to 0.5 g/L for MAB4714) with a lower level of the 6-HHA intermediate (Figure 6D). Other CARs tested showed a lower increase in this reaction.

A recent work has demonstrated that *in vitro* activity of the *N. iowensis* CAR (CAR_NOCIO) is inhibited by the formation of the co-product pyrophosphate, whose hydrolysis using an inorganic pyrophosphatase (PPase) resulted in a significant increase in

the reaction rate and product yield [25, 26, 43]. Therefore, we used the purified PPase from *E. coli* to further increase the efficiency of *in vitro* substrate conversion by CARs in the presence of NADPH and ATP regenerating systems. As shown in Figure 6E, the addition of PPase increased the reduction of 10 mM 4-HB to 1,4-BDO by all CARs with MAB4714, MAP1040, and MIM0040 showing 70 – 90% conversion (0.6 – 0.8 g/L). Even greater improvement was observed when PPase was used in the transformation of adipic acid to 1,6-HDO by purified CARs with five enzymes exhibiting more that 50% substrate conversion and MAB4714 showing up to 76% conversion (1.16 g/L) (Figure 6F). Interestingly, the addition of PPase reduced the level of the 6-HHA intermediate with the complete reduction of adipic acid to 1,6-HDO by most CARs (Figure 6F). Thus, when supplemented with cofactor regenerating systems and inorganic pyrophosphatase, purified CARs can catalyze up to 76% substrate conversion in the *in vitro* biotransformation of 4-HB and adipic acid.

3.6 *In vivo* biotransformation of 4-HB and adipic acid by *E. coli* cells expressing CARs

Continual replenishment of cofactors for CAR-catalyzed reactions can be achieved using *E. coli* cells expressing both CAR and PPT genes as biocatalysts. Previous works have already demonstrated an efficient use of engineered *E. coli* cells harboring *Nocardia* or *M. marinum* CARs for the transformation of vanillic acid to vanillin or for the synthesis of fatty alcohols and alkanes [20, 22]. In our case, *E. coli* can also provide endogenous alcohol dehydrogenases and AKRs for the reduction of aldehydes generated by CARs to alcohols, thereby eliminating the requirement for expressing PP3340 or other exogenous AKRs. Recent studies have demonstrated that *E. coli* cells express up to 13 highly active AKRs with wide substrate specificities ranging from C2 to C18 aldehydes [48, 49]. Therefore, for the *in vivo* biotransformation of 4-HB and adipic acid to diols using *E. coli* cells expressing CARs the second reduction reaction (aldehydes to alcohols) can be catalyzed by endogenous AKRs.

In this work, *E. coli* BL21(DE3) cells expressing eight different CARs (and the *B. subtilis* PPT BSU03570) produced significant amounts of 1,4-BDO (1 – 2 mM) after 6 hours of incubation in the LB medium containing 2% glucose and 10 mM 4-HB, whereas 24 h or 48 h incubations led to 50 – 95% substrate conversion by most strains (except for MCH22995) (Figure 7A). These results indicate that *E. coli* cells can efficiently reduce 4-hydroxybutanal produced by CARs to 1,4-BDO. With 10 mM adipic acid as substrate, six *E. coli* strains generated significant amounts of 6-HHA and/or 1,6-HDO after 24 h of incubation, which increased to 54–57% conversion to 6-HHA or 1,6-HDO after 48 hours of incubation (Figure 7B). The *E. coli* strains expressing MAB4714, MIM0040, MSM5586, and SRO1679 produced mostly 6-HHA as the final product with smaller amounts of 1,6-HDO (Figure 7B). In contrast, MSM5739 produced mostly 1,6-HDO, whereas MSM2956 generated an approximately equimolar mixture of both products (Figure 7B). These results indicate that in *E. coli* cells MSM5739 efficiently reduces both adipic acid and 6-HHA, whereas MAB4714 and MIM0040 are more active toward adipic acid (compared to 6-HHA). However, all CARs produced mostly or exclusively 1,6-HDO from adipic acid *in vitro* in the presence of cofactor regenerating systems and pyrophosphatase (Figure 6F) suggesting that protein expression level or intracellular conditions (cofactor regeneration) might affect activity of CARs in *E. coli* cells.

4 Conclusion

In recent years, the practical applicability of biocatalysis and enzymatic reduction using whole cells and isolated enzymes has undergone dramatic improvements rendering it a viable alternative to chemocatalysis [3, 7]. Compared to chemical reduction of carboxylic acids, their enzymatic reduction using CAR enzymes allows for catalytic processes with excellent chemoselectivity leaving other functional groups unaffected [5]. Our phylogenetic analysis revealed broad diversity of CARs with hundreds/thousands of sequences present in bacterial and fungal genomes. To date, only a few microbial CARs have been biochemically characterized with the vast majority of these enzymes remaining to be explored. In this work, we presented novel bacterial CARs with a broad substrate scope, which can be readily expressed in *E. coli*. These enzymes also tolerate the presence of additional functional groups in their substrates (oxo-, hydroxy-, amino-, and carboxyl) providing an insight into substrate binding and substituent effects. We also demonstrated the applicability of CARs for *in vitro* and *in vivo* biotransformations of 4-HB and adipic acid and good compatibility of CARs with the downstream and cofactor regenerating enzymes. Further structural and mechanistic studies of CARs from different phylogenetic groups will shed more light on their substrate selectivities and mechanisms contributing to the development of novel reductive biocatalysts for applications in synthetic organic chemistry and biotechnology.

Supplementary Material

Refer to Web version on PubMed Central for supplementary material.

Acknowledgments

We thank all members of the BioZone Centre for Applied Bioscience and Bioengineering for help in conducting experiments. This work was supported by the NSERC Strategic Network grant IBN (A.F.Y.) and the NIH grants GM094585 and GM115586 (B.N.).

Abbreviations

1,4-BDO	1,4-butanediol
1,6-HDO	1,6-hexanediol
4-HB	4-hydroxybutyrate
6-HHA	6-hydroxyhexanoic acid
10-AD	10-aminodecanoic acid
AKR	aldo-keto reductase
CAR	carboxylic acid reductase
FDH	formate dehydrogenase
polyP	inorganic polyphosphate
PPase	inorganic pyrophosphosphatase

PPK	polyphosphate kinase
PPT	phosphopantetheinyl transferase
RS	regenerating system
SEM	standard error of mean

References

1. Bozell JJ, Petersen GR. Technology development for the production of biobased products from biorefinery carbohydrates – the US Department of Energy's "Top 10" revisited. Green Chem. 2010; 12:539–554.
2. Lee JW, Kim HU, Choi S, Yi J, Lee SY. Microbial production of building block chemicals and polymers. Curr Opin Biotechnol. 2011; 22:758–767. [PubMed: 21420291]
3. Reetz MT. Biocatalysis in organic chemistry and biotechnology: past, present, and future. J Am Chem Soc. 2013; 135:12480–12496. [PubMed: 23930719]
4. Jang YS, Kim B, Shin JH, Choi YJ, et al. Bio-based production of C2-C6 platform chemicals. Biotechnol Bioeng. 2012; 109:2437–2459. [PubMed: 22766912]
5. Napora-Wijata K, Strohmeier GA, Winkler M. Biocatalytic reduction of carboxylic acids. Biotechnol J. 2014; 9:822–843. [PubMed: 24737783]
6. Alonso S, Rendueles M, Diaz M. Microbial production of specialty organic acids from renewable and waste materials. Crit Rev Biotechnol. 2015; 35:497–513. [PubMed: 24754448]
7. Bornscheuer UT, Huisman GW, Kazlauskas RJ, Lutz S, et al. Engineering the third wave of biocatalysis. Nature. 2012; 485:185–194. [PubMed: 22575958]
8. Chung H, Yang JE, Ha JY, Chae TU, et al. Bio-based production of monomers and polymers by metabolically engineered microorganisms. Curr Opin Biotechnol. 2015; 36:73–84. [PubMed: 26318077]
9. Hollmann F, Arends IWCE, Holtmann D. Enzymatic reductions for the chemist. Green Chem. 2011:2285–2314.
10. Thauer RK, Jungermann K, Decker K. Energy conservation in chemotrophic anaerobic bacteria. Bacteriol Rev. 1977; 41:100–180. [PubMed: 860983]
11. White H, Strobl G, Feicht R, Simon H. Carboxylic acid reductase: a new tungsten enzyme catalyses the reduction of non-activated carboxylic acids to aldehydes. Eur J Biochem. 1989; 184:89–96. [PubMed: 2550230]
12. Mukund S, Adams MW. The novel tungsten-iron-sulfur protein of the hyperthermophilic archaebacterium, Pyrococcus furiosus, is an aldehyde ferredoxin oxidoreductase. Evidence for its participation in a unique glycolytic pathway. J Biol Chem. 1991; 266:14208–14216. [PubMed: 1907273]
13. Gross GG, Bolkart KH, Zenk MH. Reduction of cinnamic acid to cinnamaldehyde and alcohol. Biochem Biophys Res Commun. 1968; 32:173–178. [PubMed: 4386171]
14. Li T, Rosazza JP. Purification, characterization, and properties of an aryl aldehyde oxidoreductase from Nocardia sp. strain NRRL 5646. J Bacteriol. 1997; 179:3482–3487. [PubMed: 9171390]
15. Kato N, Joung EH, Yang HC, Masuda M, Shimao M, Yanase H. Purification and characterization of aromatic acid reductase from Nocardia asteroides JCM 3016. Agric Biol Chem. 1991; 55:757–762.
16. Gross GG. Formation and reduction of intermediate acyladenylate by aryl-aldehyde. NADP oxidoreductase from Neurospora crassa. Eur J Biochem. 1972; 31:585–592. [PubMed: 4405494]
17. Li T, Rosazza JP. NMR identification of an acyl-adenylate intermediate in the aryl-aldehyde oxidoreductase catalyzed reaction. J Biol Chem. 1998; 273:34230–34233. [PubMed: 9852085]
18. He A, Li T, Daniels L, Fotheringham I, Rosazza JP. Nocardia sp. carboxylic acid reductase: cloning, expression, and characterization of a new aldehyde oxidoreductase family. Appl Environ Microbiol. 2004; 70:1874–1881. [PubMed: 15006821]

19. Venkitasubramanian P, Daniels L, Rosazza JP. Reduction of carboxylic acids by Nocardia aldehyde oxidoreductase requires a phosphopantetheinylated enzyme. J Biol Chem. 2007; 282:478–485. [PubMed: 17102130]
20. Venkitasubramanian P, Daniels L, Das S, Lamm AS, Rosazza JP. Aldehyde oxidoreductase as a biocatalyst: Reductions of vanillic acid. Enzyme Microb Technol. 2008; 42:130–137. [PubMed: 22578862]
21. Sheppard MJ, Kunjapur AM, Wenck SJ, Prather KL. Retro-biosynthetic screening of a modular pathway design achieves selective route for microbial synthesis of 4-methyl-pentanol. Nat Commun. 2014; 5:5031. [PubMed: 25248664]
22. Akhtar MK, Turner NJ, Jones PR. Carboxylic acid reductase is a versatile enzyme for the conversion of fatty acids into fuels and chemical commodities. Proc Natl Acad Sci U S A. 2013; 110:87–92. [PubMed: 23248280]
23. Duan YYP, Chen X, Liu X, Zhang R, Feng J, Wu Q, Zhu D. Exploring the synthetic applicability of a new carboxylic acid reductase from Segniliparus rotundus DSM 44985. J Mol Catalysis B: Enzymatic. 2015; 115:1–7.
24. Moura M, Pertusi D, Lenzini S, Bhan N, et al. Characterizing and predicting carboxylic acid reductase activity for diversifying bioaldehyde production. Biotechnol Bioeng. 2016; 113:944–952. [PubMed: 26479709]
25. Finnigan W, Thomas A, Cromar H, Gough B, Snajdrova R, Adams JP, Littlechild JA, Harmer NJ. Characterization of carboxylic acid reductases as enzymes in the toolbox for synthetic chemistry. ChemCatChem. 2017; 9:1–14.
26. Schwendenwein D, Fiume G, Weber H, Rudroff F, Winkler M. Selective Enzymatic Transformation to Aldehydes in vivo by Fungal Carboxylate Reductase from Neurospora crassa. Adv Synth Catal. 2016; 358:3414–3421. [PubMed: 27917101]
27. Kallio P, Pasztor A, Thiel K, Akhtar MK, Jones PR. An engineered pathway for the biosynthesis of renewable propane. Nat Commun. 2014; 5:4731. [PubMed: 25181600]
28. Kunjapur AM, Tarasova Y, Prather KL. Synthesis and accumulation of aromatic aldehydes in an engineered strain of Escherichia coli. J Am Chem Soc. 2014; 136:11644–11654. [PubMed: 25076127]
29. Sheppard MJ, Kunjapur AM, Prather KL. Modular and selective biosynthesis of gasoline-range alkanes. Metab Eng. 2016; 33:28–40. [PubMed: 26556131]
30. France SP, Hussain S, Hill AM, Hepworth LJ, Howard RM, Mulholland KR, Flitsch SL, Turner NJ. One-pot cascade synthesis of mono- and disubstituted piperidines and pyrrolidines using carboxylic acid reductase (CAR), transaminase (TA), and imine reductase (IRED) biocatalysis. ACS Catalysis. 2016; 6:3753–3759.
31. Geer LY, Domrachev M, Lipman DJ, Bryant SH. CDART: protein homology by domain architecture. Genome Res. 2002; 12:1619–1623. [PubMed: 12368255]
32. Fu L, Niu B, Zhu Z, Wu S, Li W. CD-HIT: accelerated for clustering the next-generation sequencing data. Bioinformatics. 2012; 28:3150–3152. [PubMed: 23060610]
33. Gouveia-Oliveira R, Sackett PW, Pedersen AG. MaxAlign: maximizing usable data in an alignment. BMC Bioinformatics. 2007; 8:312. [PubMed: 17725821]
34. Yamada KD, Tomii K, Katoh K. Application of the MAFFT sequence alignment program to large data – reexamination of the usefulness of chained guide trees. Bioinformatics. 2016; 32:3246–3251. [PubMed: 27378296]
35. Kuznetsova E, Proudfoot M, Gonzalez CF, Brown G, et al. Genome-wide analysis of substrate specificities of the Escherichia coli haloacid dehalogenase-like phosphatase family. J Biol Chem. 2006; 281:36149–36161. [PubMed: 16990279]
36. Heering HA, Weiner JH, Armstrong FA. Direct detection and measurement of electron relays in a multicentered enzyme: voltammetry of electrode-surface films of E. coli fumarate reductase, an iron-sulfur flavoprotein. J Am Chem Soc. 1997; 119:11628–11638.
37. Nocek B, Kochinyan S, Proudfoot M, Brown G, et al. Polyphosphate-dependent synthesis of ATP and ADP by the family-2 polyphosphate kinases in bacteria. Proc Natl Acad Sci U S A. 2008; 105:17730–17735. [PubMed: 19001261]

38. Tchigvintsev A, Singer AU, Flick R, Petit P, et al. Structure and activity of the Saccharomyces cerevisiae dUTP pyrophosphatase DUT1, an essential housekeeping enzyme. Biochem J. 2011; 437:243–253. [PubMed: 21548881]
39. Ihara M, Kawano Y, Urano M, Okabe A. Light driven CO2 fixation by using cyanobacterial photosystem I and NADPH-dependent formate dehydrogenase. PLoS One. 2013; 8:e71581. [PubMed: 23936519]
40. Stolterfoht H, Schwendenwein D, Sensen CW, Rudroff F, Winkler M. Four distinct types of E.C. 1.2.1.30 enzymes can catalyze the reduction of carboxylic acids to aldehydes. J Biotechnol. 2017 (in press).
41. Yim H, Haselbeck R, Niu W, Pujol-Baxley C, et al. Metabolic engineering of Escherichia coli for direct production of 1,4-butanediol. Nat Chem Biol. 2011; 7:445–452. [PubMed: 21602812]
42. Yu JL, Xia XX, Zhong JJ, Qian ZG. Direct biosynthesis of adipic acid from a synthetic pathway in recombinant Escherichia coli. Biotechnol Bioeng. 2014; 111:2580–2586. [PubMed: 24895214]
43. Kunjapur AM, Cervantes B, Prather KLJ. Coupling carboxylic acid reductase to inorganic pyrophosphatase enhances cell-free in vitro aldehyde biosynthesis. Biochem Eng J. 2016; 109:19–27.
44. Hummel W, Groger H. Strategies for regeneration of nicotinamide coenzymes emphasizing self-sufficient closed-loop recycling systems. J Biotechnol. 2014; 191:22–31. [PubMed: 25102236]
45. Crans DC, Kazlauskas RJ, Hirschbein BL, Wong CH, et al. Enzymatic regeneration of adenosine 5′-triphosphate: acetyl phosphate, phosphoenolpyruvate, methoxycarbonyl phosphate, dihydroxyacetone phosphate, 5-phospho-alpha-D-ribosyl pyrophosphate, uridine-5′-diphosphoglucose. Methods Enzymol. 1987; 136:263–280. [PubMed: 2446104]
46. Resnick SM, Zehnder AJ. In vitro ATP regeneration from polyphosphate and AMP by polyphosphate:AMP phosphotransferase and adenylate kinase from Acinetobacter johnsonii 210A. Appl Environ Microbiol. 2000; 66:2045–2051. [PubMed: 10788379]
47. Zhao H, van der Donk WA. Regeneration of cofactors for use in biocatalysis. Curr Opin Biotechnol. 2003; 14:583–589. [PubMed: 14662386]
48. Rodriguez GM, Atsumi S. Toward aldehyde and alkane production by removing aldehyde reductase activity in Escherichia coli. Metab Eng. 2014; 25:227–237. [PubMed: 25108218]
49. Fatma Z, Jawed K, Mattam AJ, Yazdani SS. Identification of long chain specific aldehyde reductase and its use in enhanced fatty alcohol production in E. coli. Metab Eng. 2016; 37:35–45. [PubMed: 27134112]

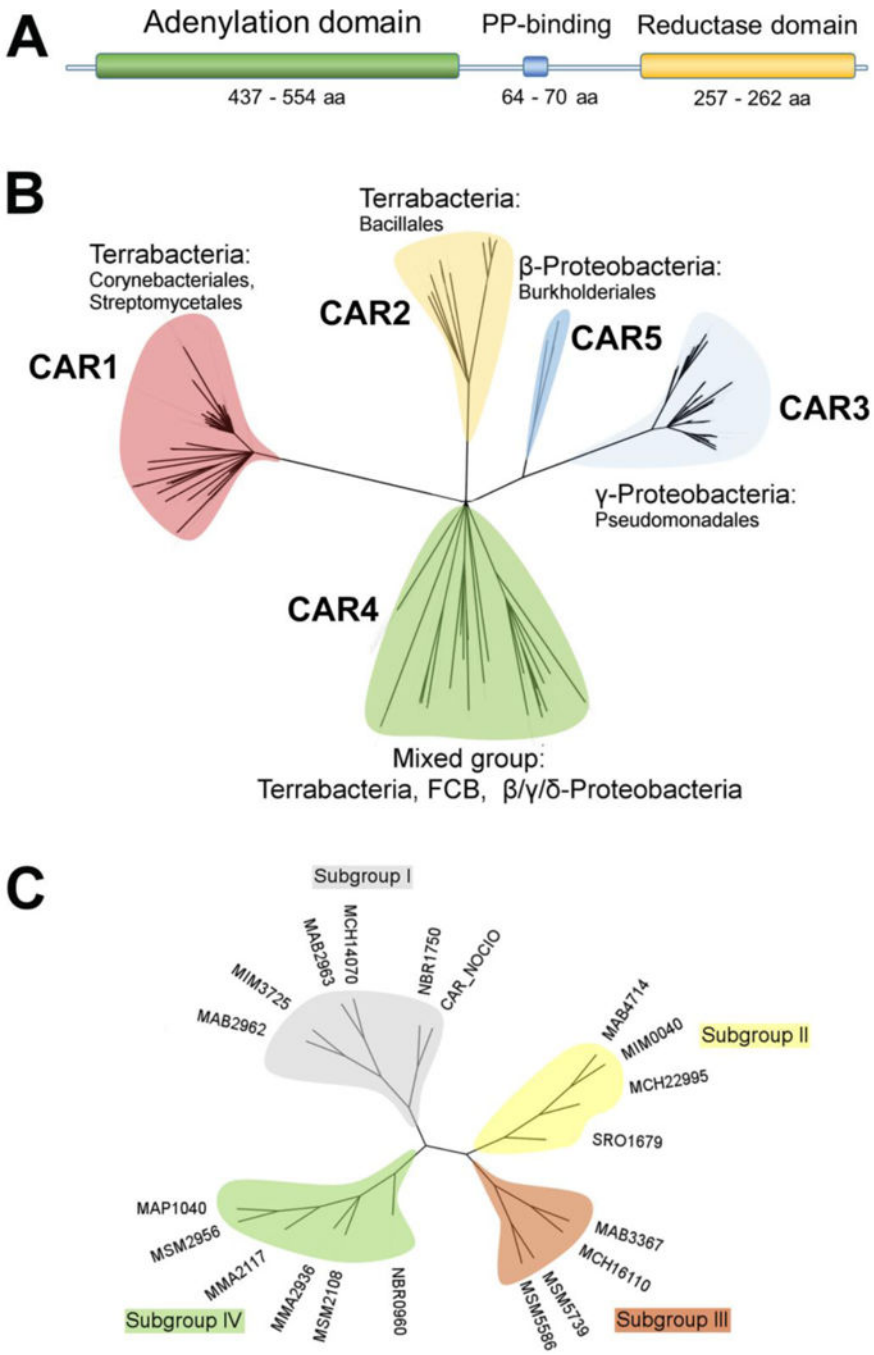

Figure 1.

Phylogenetic analysis of CARs. (A), domain organization of CAR sequences: adenylation domain (PFam PF00501), phosphopantetheine (PP) attachment site (PF00550), reductase domain (PF07793). (B), Phylogenetic tree of prokaryotic CARs showing the five monophyletic groups (CAR1-5). (C), Neighbor-joining tree of 20 bacterial CARs cloned in this work (CAR1 group). Bootstrap values for both trees were > 60%.

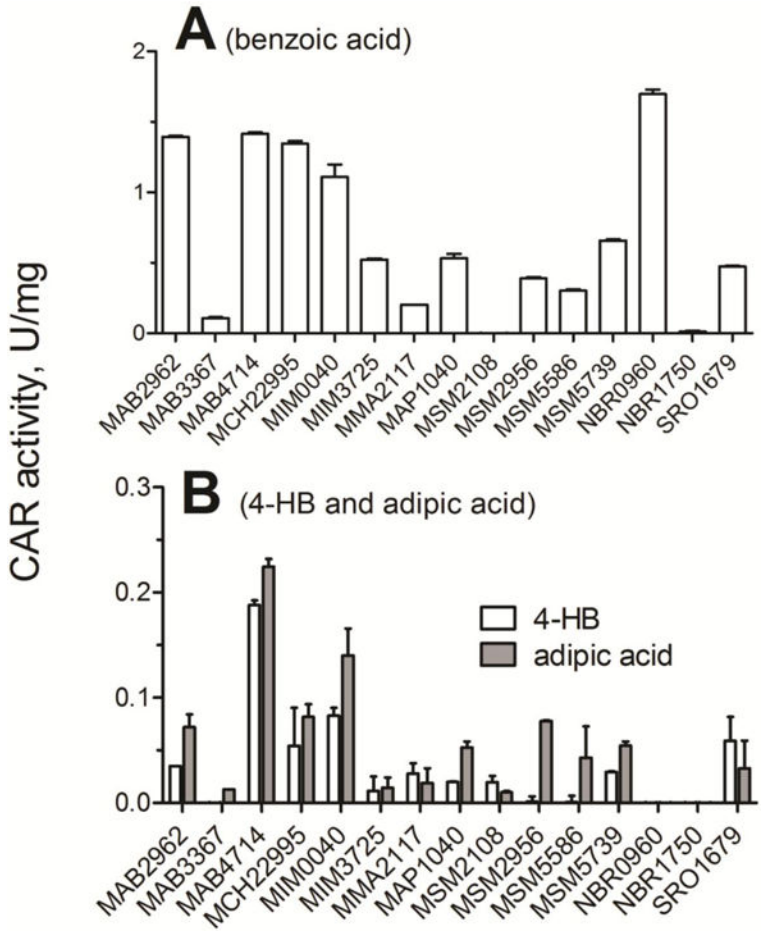

Figure 2.

Screening of purified CARs for reductase activity. (A), benzoic acid as substrate; (B), 4-HB and adipic acid as substrates. NADPH oxidation assays were performed using 10 mM substrate, 1 mM NADPH, 2.5 mM ATP, 10 mM $MgCl_2$, and 5 μg of purified CAR. Results are means ± SEM from at least three independent determinations.

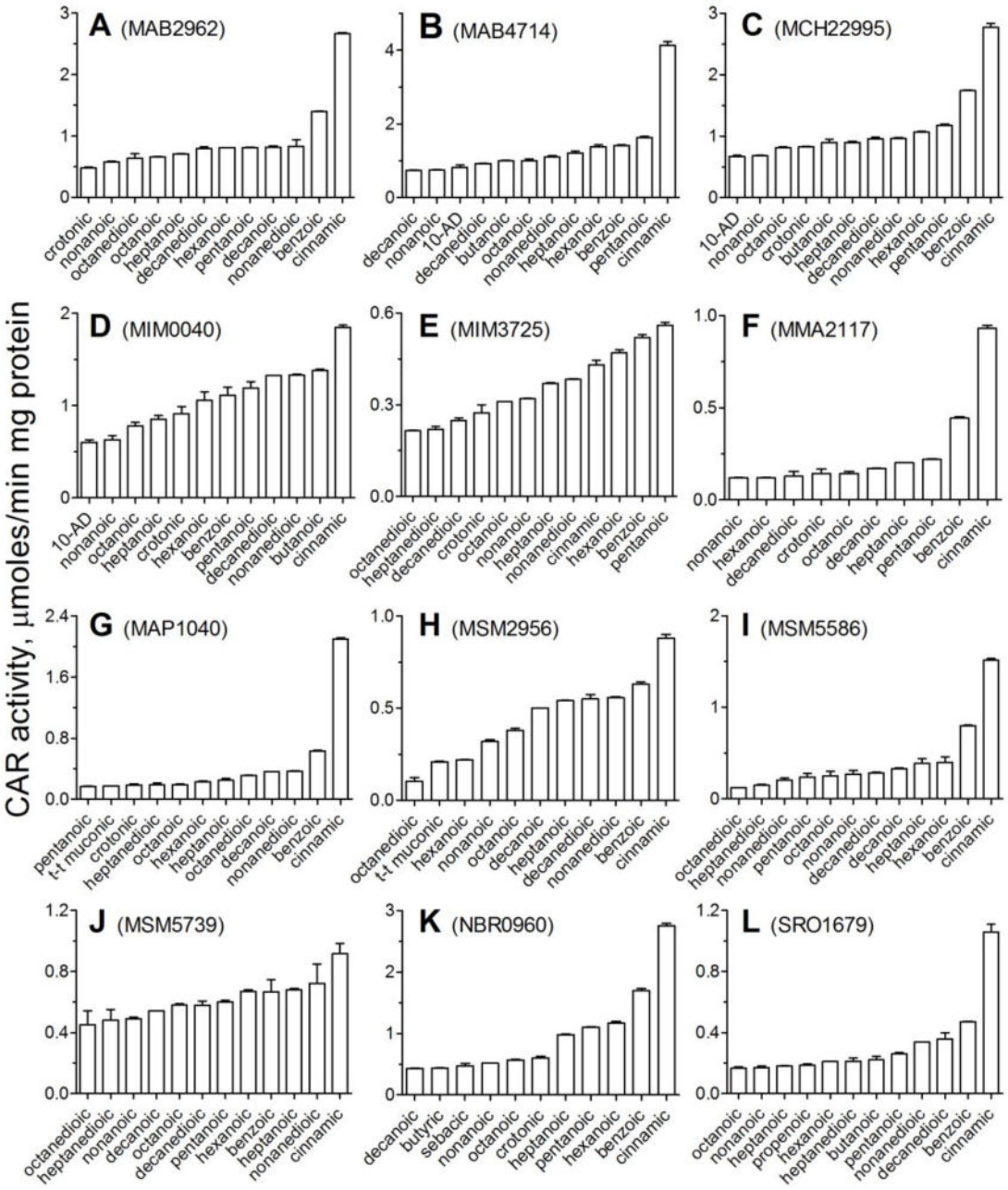

Figure 3.

Substrate profiles of 12 purified CARs. Proteins were screened for reductase activity against 87 substrates, and the best positive substrates are shown. Reactions were performed using 10 mM substrate (5 mM for decanoic acid) as described in the Experimental Section (10-AD, 10-aminodecanoic acid). Results are means ± SEM from at least three independent determinations.

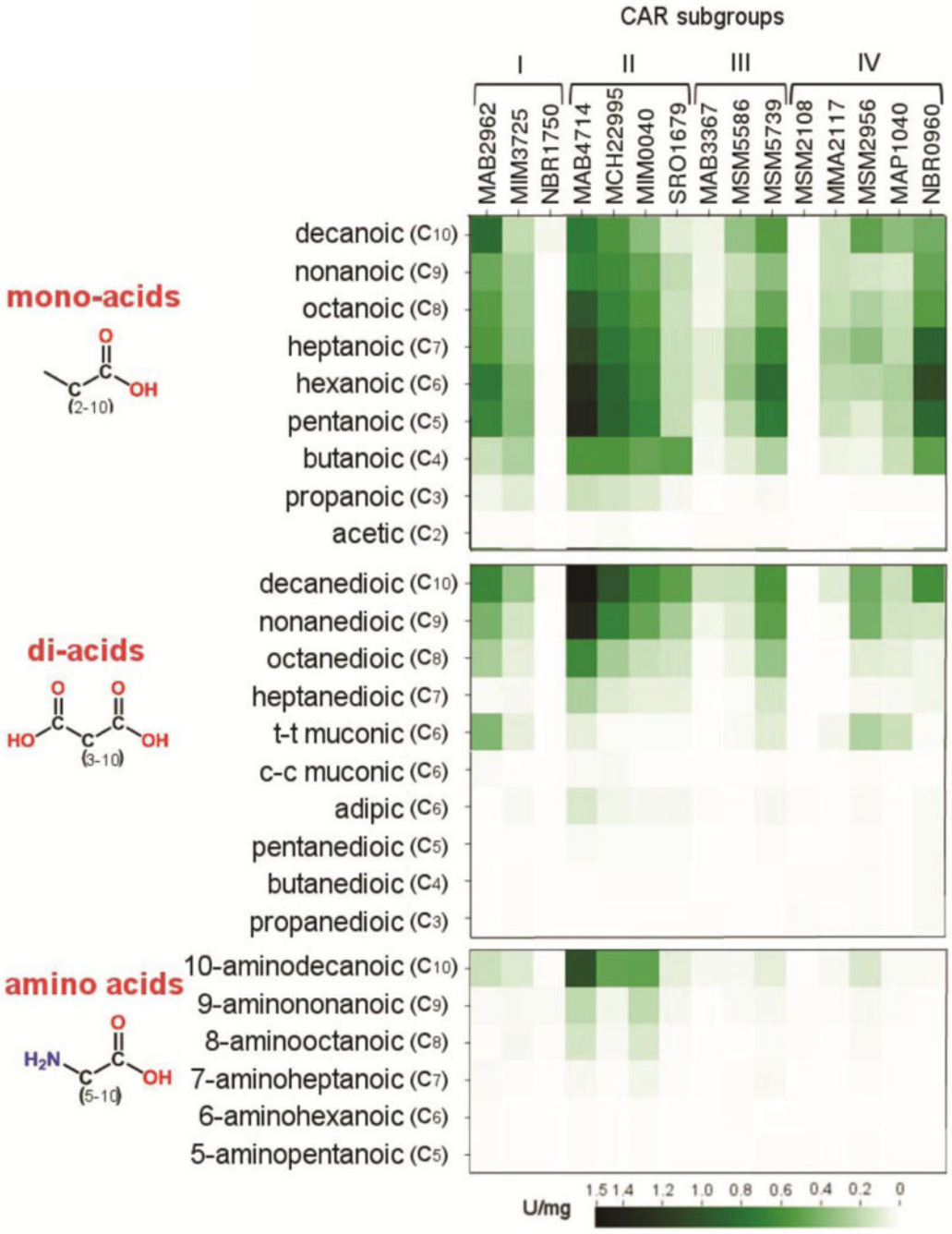

Figure 4.

Substrate preferences of 15 purified CARs: effects of the substrate chain length and second functional groups. The heat map represents CAR activities (U/mg or μmoles/min per mg protein) against the indicated substrates with the color code shown at the bottom (white color indicates no detectable activity). The heat map was generated using single matrix CIMminer (https://discover.nci.nih.gov/cimminer/home.do). Reaction conditions were as indicated in Materials and Methods.

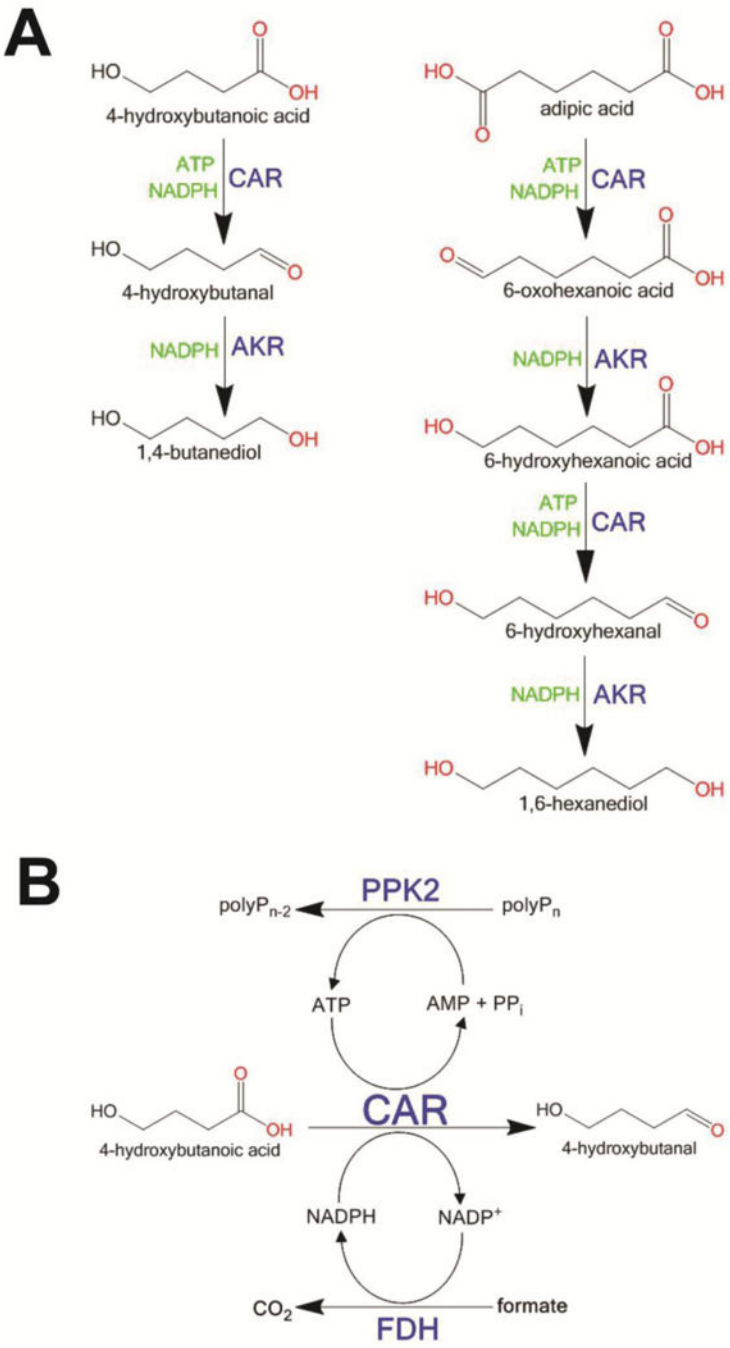

Figure 5.

Proposed biochemical reactions and cofactor regenerating systems for CARs. (A), *In vitro* biotransformation of 4-HB and adipic acid using CARs and AKRs. (B), Cofactor regenerating systems used in this work. Regeneration of ATP from AMP is catalyzed by polyphosphate kinases in the presence of polyP, whereas $NADP^+$ reduction is performed by the *Pseudomonas* formate dehydrogenase (FDH) D222Q/H224N mutant protein in the presence of formate.

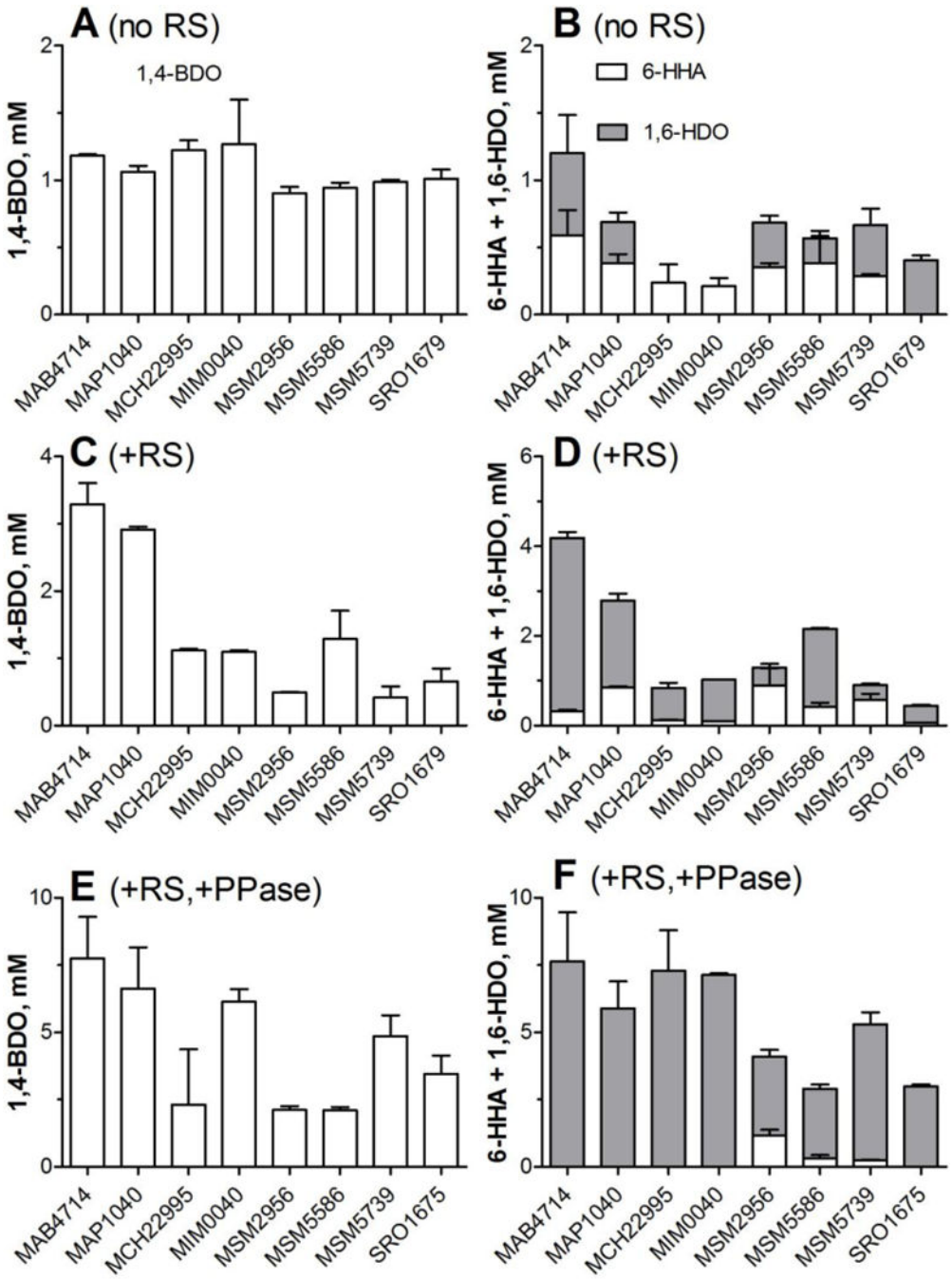

Figure 6.

In vitro transformation of 4-HB and adipic acid by purified CARs. (A, B), without cofactor regeneration (no RS); (C, D), with the regeneration of ATP and NADPH (+RS); (E, F), with cofactor regeneration in the presence of inorganic pyrophosphatase (+RS, +PPase). For reactions with adipic acid (B, D, and F), the white sections of bars show the concentration of 6-HHA, whereas the grey sections represent 1,6-HDO. Reaction mixtures contained 10 mM substrate, 80 μg of CAR, and 20 μg of AKR (PP3340), and reaction products (1,4-BDO, 6-

HHA, and 1,6-HDO) were analyzed using HPLC. Results are means ± SEM from at least three independent determinations.

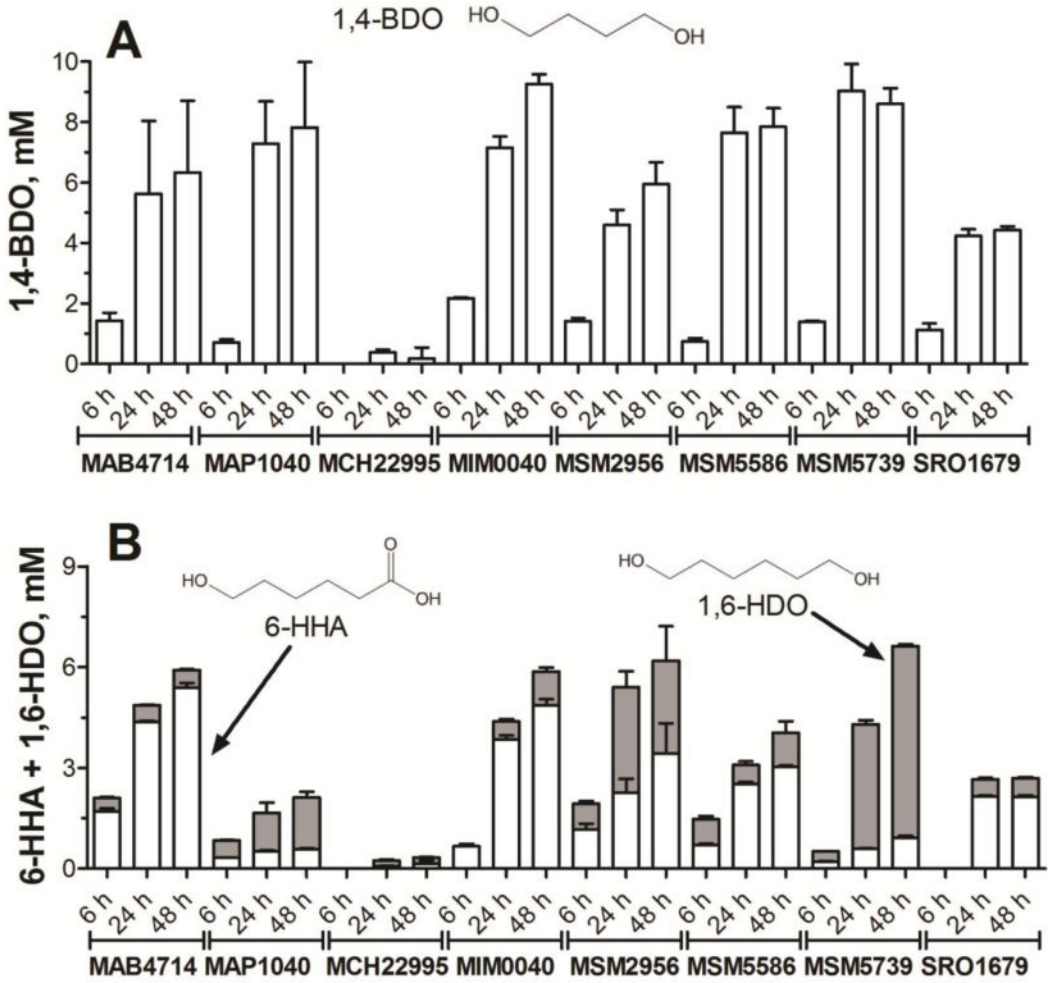

Figure 7.

In vivo transformation of 4-HB and adipic acid by *E. coli* cells expressing CARs. The *E. coli* BL21 cells over-expressing the indicated CARs (and PPT BSU03570) were grown in LB medium with 2% glucose and 10 mM 4-HB (A) or 10 mM adipic acid. Culture aliquots were collected after 6 h, 24 h, and 48 h of growth, and reaction products (1,4-BDO, 6-HHA, and 1,6-HDO) were analyzed using HPLC. For panel B, the white sections of bars show the concentration of 6-HHA, whereas the grey sections represent 1,6-HDO. Results are means ± SEM from at least three independent determinations.

Table 1

Bacterial CARs purified and screened in this work. Full protein information is presented in Suppl. Materials (Table S1.)

CAR name	Organism	Comments	Reference
1. MAB2962	*M. abscessus*	expressed/soluble/active	this work
2. MAB2963	*M. abscessus*	no expression	this work
3. MAB3367	*M. abscessus*	expressed/soluble/inactive	this work
4. MAB4714	*M. abscessus*	expressed/soluble/active	this work
5. MAP1040	*M. avium*	expressed/soluble/active	this work
5. MCH14070	*M. chelonae*	no expression	this work
6. MCH16110	*M. chelonae*	no expression	this work
7. MCH22995	*M. chelonae*	expressed/soluble/active	this work
8. MIM0040	*M. immunogenum*	expressed/soluble/active	this work
9. MIM3725	*M. immunogenum*	expressed/soluble/active	this work
10. MMA2117	*M. marinum*	expressed/soluble/active	[22]
11. MMA2936	*M. marinum*	no expression	this work
13. MSM2108	*M. smegmatis*	expressed/soluble/inactive	this work
14. MSM2956	*M. smegmatis*	expressed/soluble/active	this work
15. MSM5586	*M. smegmatis*	expressed/soluble/active	[25]
16. MSM5739	*M. smegmatis*	expressed/soluble/active	this work
17. NBR0960	*N. brasiliensis*	expressed/soluble/active	this work
18. NBR1750	*N. brasiliensis*	expressed/soluble/inactive	this work
19. CAR_NOCIO	*N. iowensis*	no expression	[19]
20. SRO1679	*S. rotundus*	expressed/soluble/active	[23]

Table 2

Kinetic parameters of purified CARs with different substrates.[a]

Proteins	Variable substrate	K_m, mM	k_{cat}, s^{-1}	k_{cat}/K_m, $M^{-1}s^{-1}$
MAB4714	ATP[a]	0.047 ± 0.004	6.11 ± 0.11	1.3×10^5
	NADPH[b]	0.039 ± 0.005	8.03 ± 0.27	2.1×10^5
	benzoic acid	0.724 ± 0.004	4.47 ± 0.15	0.6×10^4
	4-hydroxybutanoic acid	35.9 ± 3.1	2.13 ± 0.07	0.6×10^2
	adipic acid	23.9 ± 4.5	1.88 ± 0.13	0.8×10^2
	6-hydroxyhexanoic acid	2.62 ± 0.03	2.64 ± 0.13	1.0×10^3
MSM5739	ATP	0.18 ± 0.01	1.60 ± 0.02	0.9×10^4
	NADPH	0.003±0.001	0.74±0.03	0.27×10^3
	benzoic acid	7.25 ± 0.60	3.74 ± 0.15	0.5×10^3
	4-hydroxybutanoic acid	67. 1 ± 8.8	0.66 ± 0.03	0.98 × 10
	adipic acid	115. 5 ± 28.2	2.59 ± 0.39	0.2×10^2
	6-hydroxyhexanoic acid	8.33 ± 0.73	1.21 ± 0.04	1.5×10^2
MAP1040	ATP	0.21 ± 0.02	1.99 ± 0.04	0.9×10^4
	NADPH	0.006±0.002	1.60±0.10	0.27×10^3
	benzoic acid	1.23 ± 0.09	2.92 ± 0.06	2.4×10^3
	4-hydroxybutanoic acid	69.9 ± 8.0	0.75 ± 0.04	1.1 × 10
	adipic acid	52.8 ± 9.6	0.78 ± 0.07	1.5 × 10
	6-hydroxyhexanoic acid	70.1 ± 7.0	2.91 ± 0.19	0.4×10^2
SRO1679	ATP	0.56 ± 0.13	1.40 ± 0.09	2.5×10^3
	NADPH	0.016±0.005	3.46±0.30	0.21×10^3
	benzoic acid	0.33 ± 0.06	2.27 ± 0.09	0.7×10^4
	4-hydroxybutanoic acid	35.5 ± 4.1	0.42 ± 0.02	1.2 × 10
	adipic acid	28.4 ± 6.7	0.39 ± 0.04	1.4 × 10
MIM0040	ATP	0.12±0.02	22.64±0.71	0.19×10^3
	NADPH	0.050±0.006	18.65±0.36	0.37×10^3
	benzoic acid	0.39 ± 0.03	7.83 ± 0.13	2.0×10^4
	4-hydroxybutanoic acid	80.3 ± 5.4	1.00 ± 0.03	1.2 ×10
	adipic acid	44.4 ± 10.3	2.3 ± 0.3	5.2 × 10
MAB2962	ATP	0.32 ± 0.05	3.78 ± 0.15	1.2×10^4
	NADPH	0.015±0.002	7.13±0.29	0.46×10^3
	benzoic acid	1.31 ± 0.06	6.99 ± 0.09	0.5×10^4

[a]Each value represents mean ± SEM from at least three experiments.

[b]With 2 mM benzoic acid as substrate.